Shaoxin Li, Wei Kan*, Bing Zhao*, Ting Liu, Yue Fang, Liming Bai and Liyan Wang

A fluorescent pH probe for an aqueous solution composed of 7-hydroxycoumarin, Schiff base and phenanthro[9,10-*d*]imidazole moieties (PICO)

https://doi.org/10.1515/hc-2017-0174
Received August 7, 2017; accepted January 8, 2018; previously published online March 24, 2018

Abstract: The pH fluorescent probe 7-hydroxy-4-methyl-8-(((2-(1-phenyl-1*H*-phenanthro[9,10-*d*]imidazol-2-yl)phenyl)imino)methyl)-2*H*-chromen-2-one (PICO) contains a donor–π–acceptor (D–π–A) conjugated system. The 'off–on' probe PICO has a pKa value of 8.01 and its fluorescence intensity is enhanced with increasing pH.

Keywords: off–on; *o*-hydroxycoumarin; phenanthro[9,10-*d*]imidazole; pH probe; tautomerism.

Introduction

Intracellular pH (pH_i) regulates various functions of many organelles and plays vital roles in cellular events [1], including proliferation and apoptosis, cell cycle control, cell adhesion and endocytosis [2, 3]. In diverse prokaryotic species and different subcellular compartments of eukaryotic cells, pH_i can vary from highly acidic to basic values [4, 5]. Abnormal pH_i values in organelles are often associated with cellular dysfunction and affect human physiology, which is related to many diseases such as cancer [6] and Alzheimer's disease [7]. Therefore, monitoring the pH changes inside live cells is crucial to understand the cellular functions and biological and pathological processes. The use of fluorescent pH probes are the most successful approaches due to their nondestructive character, high sensitivity and high specificity [8, 9]. Many excellent pH probes for lysosomes (pH 4.5–5.0) [10–14] or cytosol (pH 6.8–7.4) [15–17] have been obtained based on the mechanism of photoinduced electron transfer (PET), internal charge transfer (ICT) and Förster resonance energy transfer (FRET).

***Corresponding authors: Wei Kan and Bing Zhao,** Chemistry and Chemical Engineering Institute, Qiqihar University, Qiqihar 161006, China, e-mail: 297133530@qq.com (W. Kan); zhao_submit@aliyun.com (B. Zhao)
Shaoxin Li, Ting Liu, Yue Fang, Liming Bai and Liyan Wang: Chemistry and Chemical Engineering Institute, Qiqihar University, Qiqihar 161006, China

The pH sensors based on conjugated Schiff bases have been paid increasing attention due to tautomerism from phenol-imine to ketone-amine forms [18] and their photochromic and thermochromic properties [19]. Among these, Schiff bases containing a hydroxy group are of a special interest [20–26] because of their characteristic property to form the ionic N^+-H…O^- hydrogen bond [19]. In continuation of our studies on pH fluorescent probes, a new pH sensitive compound 7-hydroxy-4-methyl-8-(((2-(1-phenyl-1*H*-phenanthro[9,10-*d*]imidazol-2-yl)phenyl)imino)methyl)-2*H*-chromen-2-one (PICO) was synthesized as an ICT fluorescent probe which contains *o*-hydroxycoumarin as an electron donor (D) and phenanthro[9,10-*d*]imidazole as an electron acceptor (A) mutually conjugated through Schiff base (Scheme 1). Changes in absorption and fluorescence properties of the probe PICO are observed with changes in pH.

Results and discussion

The straightforward synthesis of PICO is shown in Scheme 1. As can be seen from the proton nuclear magnetic resonance (^{1}H NMR) spectrum (see Experimental), a single peak at 9.12 ppm is due to the presence of the imino group and the sharp signal at 14.14 ppm can be assigned to the hydroxy group. This signal is located considerably downfield compared to the normal hydroxy proton resonance, which can be a result of the intramolecular hydrogen bond between the phenol group and the adjacent N atoms of the imino group and the imidazole ring.

Figure 1 shows the UV-Vis absorption spectra of PICO at various pH values. Two absorption peaks around 300 nm and 365 nm can be seen. Under strong acidic conditions (pH 2.21), a weak absorption peak is located around 300 nm. With increases in pH, the maximum absorption peak of PICO becomes stronger and is gradually shifted to around 360 nm. Furthermore, the isosbestic point at 335 nm can be assigned to the π–π^* transition of C=N and C=C functions. These results are consistent with the dominance of the enol-imine form under neutral or weakly basic conditions.

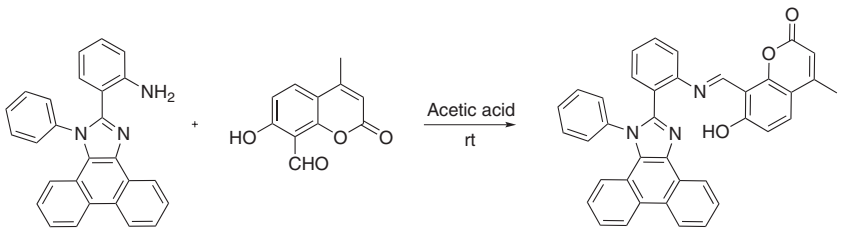

Scheme 1 Synthetic route to PICO.

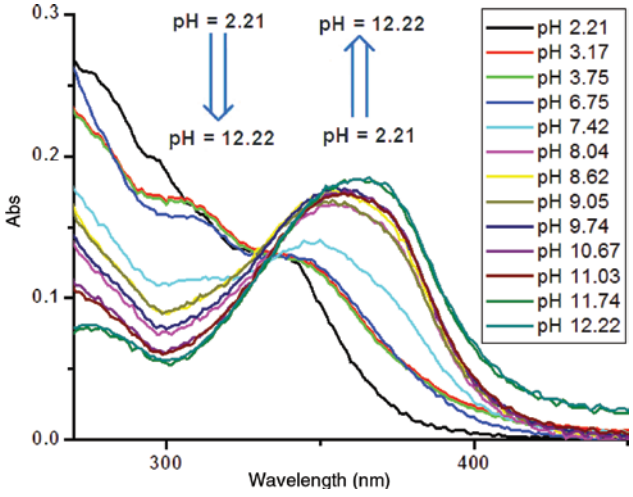

Figure 1 Absorption spectra of PICO as a function of pH.

Subsequently, the fluorescence spectra of PICO as a function of pH were investigated (Figure 2) using the isosbestic point excitation wavelength at 335 nm. The emission spectra of PICO are sensitive to pH changes with an 'off–on' switching profiles. In strongly acidic solution (pH 2.21), the fluorescence spectrum has a weak maximum emission band at 500 nm with the fluorescence quantum yield Φ of 0.024. When the acidity changes to neutral conditions (pH 7.42), the maximum emission peak of PICO in fluorescence spectrum shows a huge shift from 500 nm to 450 nm. It can be suggested that the 50-nm blue shift is the result of deprotonation of PICO with a concomitant fluorescence enhancement. Under the pH conditions of 12.22, the fluorescence quantum yield Φ is 0.43 with the maximum fluorescence intensity. It can be suggested that the increase of fluorescence intensity is a result of the disruption of the intramolecular hydrogen bond because of the deprotonation of the hydroxy group. In this situation, the oxygen anion is a strong electron donor which also alters the ICT effect and causes the fluorescence emission shift. Meanwhile, the titration curve (inset in Figure 2A) exhibits distinct pH-dependent fluorescence changes in this range, and the maximum fluorescence enhancement factor (F_{max}/F_{min}) of PICO is 50-fold (calculated with the fluorescence intensity at 450 nm). The sigmoidal fitting yielded a pKa value of 8.01 and there is a good linearity between emission and pH in this range with R^2 value of 0.9909 (Figure 2B).

Considering a possible binding of PICO with metal ions and anions, which would cause a possible interference with pH monitoring, its selectivity to pH in the presence of metal ions (Co^{2+}, Cr^{3+}, Cd^{2+}, Fe^{3+}, Zn^{2+}, Cu^{2+}, Hg^{2+}, Ni^{2+}, Al^{3+}, Ba^{2+}, Pb^{2+}, Na^+, K^+, Ca^{2+}, Ag^+, Mg^{2+}, 100 μM) and anions (I^-, Cl^-, Br^-, CO_3^{2-}, HCO_3^-, SO_4^{2-}, NO_2^-, AcO^-, $H_2PO_4^-$,

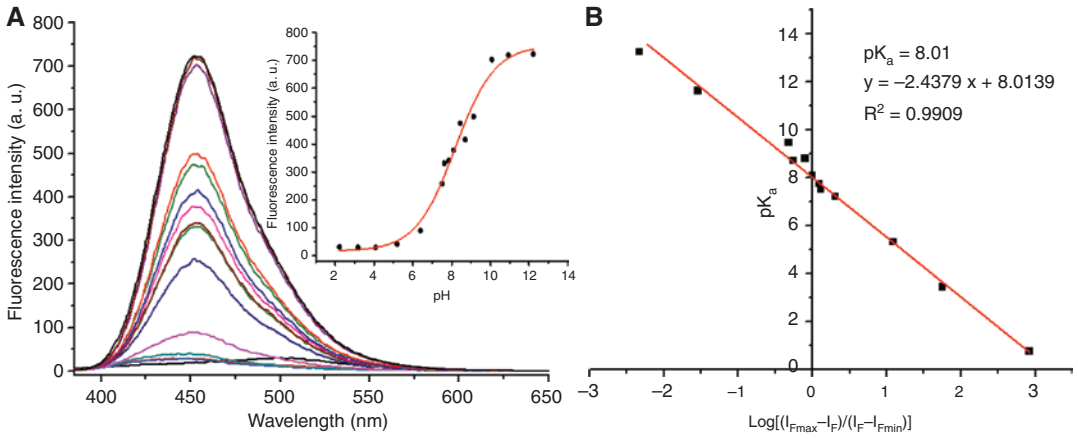

Figure 2 (A) Fluorescence spectra of PICO as a function of pH; the inset shows the fluorescence titration of PICO. (B) The sigmoidal fitting plot for fluorescence titration of PICO against pH.

HPO_4^{2-}, BrO_3^-, NO_3^-, SO_2^-, HSO_3^-, F^-, and SCN^-, 100 μM) were investigated. Figure 3A shows fluorescence intensity changes of PICO in the presence of different metal ions at pH 3.1 and 7.4. The fluorescence intensity of PICO is not affected by the addition of any metal ion under each pH condition. In a similar way, the fluorescence intensity of PICO in the presence of anions is not affected (Figure 3B). These results show excellent selectivity response of PICO in the presence of background metal ions or anions across a wide pH range.

The stability of PICO (10 μM) was tested by measuring the fluorescent response for 3 h under different pH conditions. Figure 4A shows fluorescence at pH 12.2, 7.4 and 2.2 at room temperature. The results show that fluorescence of PICO is stable over time. Reversibility of response is another important parameter to assess the performance of a fluorescence probe. The pH value was modulated back and forth 5 times between 3.1 and 12.2 by the addition of HCl (0.1 M) and NaOH (0.1 M). As shown in Figure 4B, the fluorescence changes are fully reversible in the whole pH range, which means that PICO exhibits a fully reversible response to pH.

It can be suggested that PICO exists in various tautomeric forms as shown in Scheme 2. The enol form **1** is present under neutral conditions and is transformed under basic conditions to the enol form **2** with the oxygen-centered anion. This suggestion is consistent with the ICT effect on the fluorescence change. The enol form **2** with the oxygen anion is the precursor to the stable keto structure. The density functional theory (DFT) calculations for enol and ketone tautomers, obtained at the B3LYP/6-31G* level using the B3LYP/6-31G(d) level of the Guassian 09 program, strongly support this conclusion. The calculated band gaps in water between the highest occupied molecular orbital (HOMO) and the lowest unoccupied molecular orbital (LUMO) of enol and ketone forms are 3.18 eV and 3.04 eV, respectively. Thus, the energy gap between the HOMO and LUMO of the ketone form is only slightly

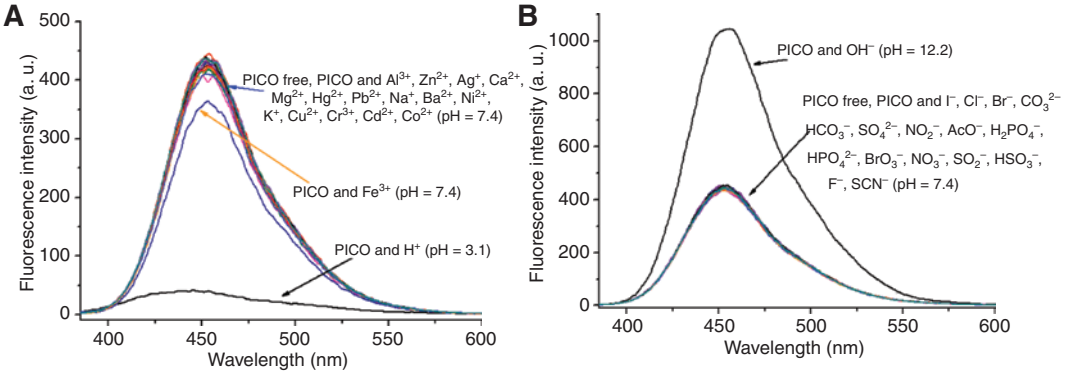

Figure 3 (A) Effect of metal ions (100 μM, Co^{2+}, Cr^{3+}, Cd^{2+}, Fe^{3+}, Zn^{2+}, Cu^{2+}, Hg^{2+}, Ni^{2+}, Al^{3+}, Ba^{2+}, Pb^{2+}, Na^+, K^+, Ca^{2+}, Ag^+, and, Mg^{2+}) on the fluorescence intensity of PICO (10 μM) at pH values of 3.1 and 7.4. (B) Effect of anions (100 μM, I^-, Cl^-, Br^-, CO_3^{2-}, HCO_3^-, SO_4^{2-}, NO_2^-, AcO^-, $H_2PO_4^-$, HPO_4^{2-}, BrO_3^-, NO_3^-, SO_2^-, HSO_3^-, F^-, SCN^-) on the fluorescence intensity of PICO (10 μM) at pH values of 7.4 and 12.2.

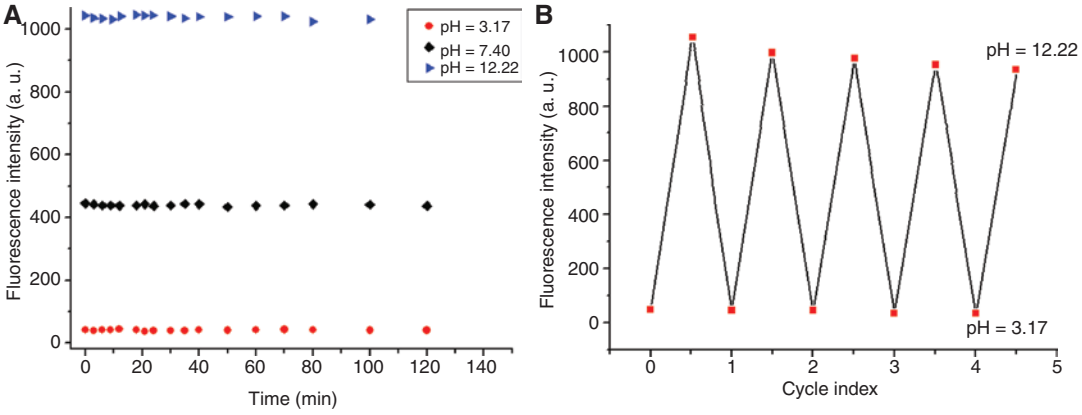

Figure 4 (A) The fluorescence intensities of PICO (10 μM) at pH 3.1, 7.4 and 12.2 over a 2-h time course. (B) Reversibility of the fluorescence intensities of PICO between pH 3.1 and 12.2.

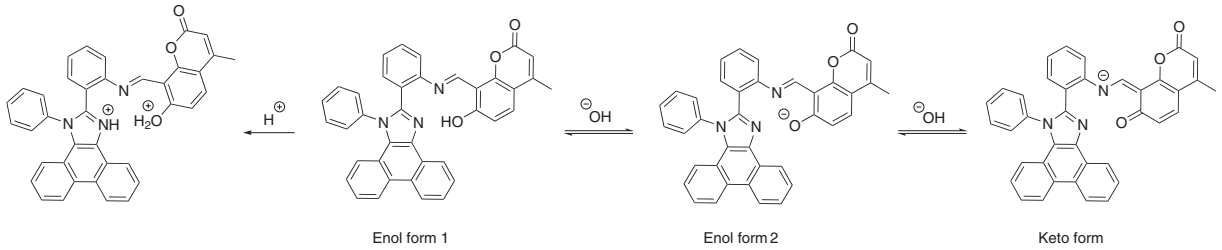

Scheme 2 A plausible equilibrium between different forms of PICO.

smaller than that of the enol form. The energy parameters also reveal that the ketone form is more stable than the enol form in DMF as well.

Conclusion

PICO is a new 'off–on' pH probe for aqueous solutions. Its pH response is not disturbed by the presence of common cations and anions. The tautomeric change between enol and keto forms was studied by ^{1}H NMR spectroscopy and DFT calculation.

Experimental

The substrates 2-(1-phenyl-1*H*-phenanthro[9,10-*d*]imidazol-2-yl)aniline and 7-hydroxy-4-methyl-2-oxo-2*H*-chromene-8-carbaldehyde were prepared as previously reported [27].

N,*N*-Dimethylformamide (DMF) was distilled over calcium hydride. Other commercial solvents were of analytical grade and used without further purification. To maintain constant pH values, the experiments were performed in water/DMF (9:1, v/v) solutions in the presence of ammonia/ammonium chloride buffer (pH > 9) and 4-(2-hydroxyethyl)1-piperazineethane sulfonic acid (HEPES) buffer (pH < 9.0 or pH 7.4). All pH measurements were made with a Sartorius PB-10 digital pH-meter. Absorption and fluorescence spectra were recorded on a TU–1901 UV-Vis spectrometer and a Perkin-Elmer LS55 fluorescence spectrophotometer, respectively.

Synthesis of PICO

A mixture of 0.77 g (2.00 mmol) of 2-(1-phenyl-1*H*-phenanthro[9,10-*d*]imidazol-2-yl)aniline and 0.41 g (2.00 mmol) of 7-hydroxy-4-methyl-2-oxo-2*H*-chromene-8-carbaldehyde in 20 mL of acetic acid was stirred for 30 min at room temperature under nitrogen atmosphere, then adjusted to pH 9.0 with a 5% aqueous solution of NaOH. The resultant precipitate was filtered and crystallized twice from a mixture of ethyl acetate and hexanes: yellow solid; yield 84%; mp 270–273°C; infrared (IR) (KBr): 3061, 1737, 1615, 1597, 1497, 1452, 753, 698 cm^{-1}; ^{1}H NMR (600 MHz, DMSO-d_6): δ 14.14 (s, 1H), 9.12 (s, 1H), 8.93 (m, 2H), 8.85(d, 1H, J = 8 Hz), 7.76 (t, 1H, J = 7 Hz), 7.72–7.69 (m, 2H), 7.65–7.63 (m, 2H), 7.57 (t, J = 8 Hz, 2H), 7.51 (t, J = 7 Hz, 1H), 7.47 (t, J = 8 Hz, 2H), 7.43 (d, 2H, J = 8 Hz), 7.36 (m, 2H), 7.13 (d, 1H, J = 8 Hz), 6.70 (d, 1H, J = 9.0 Hz), 6.26 (s, 1H), 2.37 (s, 3H); carbon-13 nuclear magnetic resonance (^{13}C NMR) (150 MHz, DMSO-d_6): δ 164.9, 159.5, 157.8, 154.5, 149.8, 146.8, 137.7, 137.0, 132.6, 131.7, 131.1, 130.2, 128.9, 128.8, 128.1, 128.0, 127.5, 127.3, 127.1, 127.1, 126.7, 126.2, 125.8, 125.0, 124.1, 122.8, 122.7, 120.7, 118.9, 114.4, 111.6, 111.0, 106.9, 40.5. Anal. Calcd for $C_{38}H_{25}N_3O_3$: C, 79.99; H, 4.26; N, 7.24. Found: C, 79.84; H, 4.41; N, 7.35.

Absorption and fluorescence pH titrations

The UV-Vis and fluorescence pH titrations of PICO were carried out in aqueous DMF (9:1, pH 7.4) in the presence of HEPES buffer. A stock solution of PICO (1.0 mM) was prepared in distilled DMF and diluted to 10 μM with water/DMF solution (9:1, pH 7.4). The pH values were controlled by the addition of HCl (0.1 M) or NaOH (0.1 M) solution. The ammonia/ammonium chloride buffer (pH > 9) and HEPES buffer (pH < 9.0, pH 7.4) were used to obtain different pH values. The fluorescence spectroscopic measurements were performed with both excitation and emission bandwidths of 10 nm. All spectroscopic experiments were carried out at room temperature.

Calculation of quantum yields

The quantum yields of PICO at pH of 3.1 and 12.2 were determined by using quinolinium hydrogen sulfate (Φ_R = 0.54 in methanol) as a reference. The values were calculated according to the equation (1), where Φ and Φ_{std} are the quantum yields, A and A_{std} are the absorbance at the excitation wavelengths, I and I_{std} are the integrated emission intensities for the unknown and the standard samples, respectively.

$$\Phi = \Phi_{std}\left(\frac{A_{std}}{A}\right)\left(\frac{I}{I_{std}}\right) \quad (1)$$

Computational methods

The energy levels of the HOMO and LUMO for both enol and ketone forms were calculated using the Gaussian 09 program package. The geometric and electronic structures of molecules were determined with the DFT method. In each optimization, the vibrational

frequencies were calculated for all optimized structures with stable geometries. The B3LYP functional and the 6–311+G (d,p) basis sets were used in the calculations.

Acknowledgments: This work was supported by the Natural Science Foundation of China (21506106) and the Natural Science Foundation of Heilongjiang Province (B201314), the Foundation of Heilongjiang Education Bureau (135209209, 135209220, LTSW201735) and the Qiqihar University Graduate Innovation Fund (YJSCX2016-ZD07).

References

[1] Martinez-Zaguilln, R.; Chinnock, B. F.; Wald-Hopkins, S.; Bernas, M.; Way, D.; Weinand, M.; Witte, M. H.; Gillies, R. J. [Ca^{2+}] and pH in homeostasis in kaposi sarcoma cells. *Cell Physiol. Biochem.* **1996**, *6*, 169–184.

[2] Han, J. Y.; Burgess, K. Fluorescent indicators for intracellular pH. *Chem. Rev.* **2010**, *110*, 2709–2728.

[3] Fan, J.; Lin, C.; Li, H.; Zhan, P.; Wang, J.; Cui, S.; Hu, M.; Chen, G.; Peng, X. A ratiometric lysosomal pH chemosensor based on fluorescence resonance energy transfer. *Dyes Pigm*. **2013**, *99*, 620–626.

[4] Miksa, M.; Komura, H.; Wu, R.; Shah, K. G.; Wang, P. A novel method to determine the engulfment of apoptotic cells by macrophages using phrodo succinimidyl ester. *J. Immunol. Methods* **2009**, *342*, 71–77.

[5] Chang, S.; Wu, X.; Li, Y.; Niu, D.; Gao, Y.; Ma, Z.; Gu, J.; Zhao, W.; Zhu, W.; Tian, H.; et al. A pH-responsive hybrid fluorescent nanoprobe for real time cell labeling and endocytosis tracking. *Biomaterials* **2013**, *34*, 10182–10190.

[6] Kim, H. J.; Heo, C. H.; Kim, H. M. Benzimidazole-based ratiometric two-photon fluorescent probes for acidic pH in live cells and tissues. *J. Am. Chem. Soc*. **2013**, *135*, 17969–17977.

[7] Sjöholm, J.; Havelius, K. G. V.; Mamedov, F.; Styring, S. Effects of pH on the S-3 state of the oxygen evolving complex in photosystem II probed by EPR split signal induction. *Biochemistry* **2010**, *49*, 9800–9808.

[8] Liu, W.; Sun, R.; Ge, J.; Xu, Y.; Xu, Y.; Lu, J.; Itoh, I.; Ihara, M. Reversible near-infrared pH probes based on benzo[a]phenoxazine. *Anal. Chem*. **2013**, *85*, 7419–7425.

[9] Wang, R.; Yu, C.; Yu, F.; Chen, L. Molecular fluorescent probes for monitoring pH changes in living cells. *Trac-Trend. Anal. Chem*. **2010**, *29*, 1004–1013.

[10] Guo, J.; Xiong, S.; Wu, X.; Shen, J.; Chu, P. In situ probing of intracellular pH by fluorescence from inorganic nanoparticles. *Biomaterials* **2013**, *34*, 9183–9189.

[11] Woods, M.; Sherry, A. D. Synthesis and luminescence studies of aryl substituted tetraamide complexes of europium (III): a new approach to pH responsive luminescent europium probes. *Inorg. Chem*. **2003**, *42*, 4401–4408.

[12] Pal, R.; Parker, D. A single component ratiometric pH probe with long wavelength excitation of europium emission. *Chem. Commun*. **2007**, *5*, 474–476.

[13] Moore, J. D.; Lord, R. L.; Cisneros, G. A.; Allen, M. J. Concentration-independent pH detection with a luminescent dimetallic Eu (III)-based probe. *J. Am. Chem. Soc.* **2012**, *134*, 17372–17375.

[14] Liu, L.; Guo, P.; Chai, L.; Shi, Q.; Xu, B.; Yuan, J.; Wang, X.; Shi, X.; Zhang, W. Fluorescent and colorimetric detection of pH by a rhodamine-based probe. *Sens. Actuator. B Chem*. **2014**, *194*, 498–502.

[15] Lv, H.; Huang, S.; Zhao, B.; Miao, J. A new rhodamine B-based lysosomal pH fluorescent indicator. *Anal. Chim. Acta* **2013**, *788*, 177–182.

[16] Xu, Y.; Jiang, Z.; Xiao, Y.; Bi, F.; Miao, J.; Zhao, B. A new fluorescent pH probe for extremely acidic conditions. *Anal. Chim. Acta* **2014**, *820*, 146–151.

[17] Yang, Y.; Lowry, M.; Xu, X.; Escobedo, J. O.; Sibrian-Vazquez, M.; Wong, L.; Schowalter, C. M.; Jensen, T. J.; Fronczek, F. R.; Warner, I. M.; et al. Seminaphthofluorones are a family of water-soluble, low molecular weight, NIR-emitting fluorophores. *Proc. Natl. Acad. Sci. USA* **2008**, *105*, 8829–8834.

[18] Lee, L. G.; Berry, G. M.; Chen, C. H. Vita blue: a new 633-nm excitable fluorescent dye for cell analysis. *Cytometry* **1989**, *10*, 151–164.

[19] Adie, E. J.; Kalinka, S.; Smith, L.; Francis, M. J.; Marenghi, A.; Cooper, M. E.; Briggs, M.; Michael, N. P.; Milligan, G.; Game, S. A pH-sensitive fluor, CypHer 5, used to monitor agonist-induced G protein-coupled receptor internalization in live cells. *Biotechniques* **2002**, *3*, 1152–1156.

[20] McMahon, B. K.; Pal, R.; Parker, D. A bright and responsive europium probe for determination of pH change within the endoplasmic reticulum of living cells. *Chem. Commun*. **2013**, *49*, 5363–5365.

[21] Gui, R.; An, X.; Huang, W. An improved method for ratiometric fluorescence detection of pH and Cd^{2+} using fluorescein isothiocyanate–quantum dots conjugates. *Anal. Chim. Acta* **2013**, *767*, 134–140.

[22] Tang, B.; Yu, F.; Li, P.; Tong, L.; Duan, X.; Xie, T.; Wang, X. A near-infrared neutral pH fluorescent probe for monitoring minor pH changes: imaging in living HepG2 and HL-7702 cells. *J. Am. Chem. Soc*. **2009**, *131*, 3016–3023.

[23] Fan, L.; Liu, Q.; Lu, D.; Shi, H.; Yang, Y.; Li, Y.; Dong, C.; Shuang, S. A novel far-visible and near-infrared pH probe for monitoring near-neutral physiological pH changes: imaging in live cells. *J. Mater. Chem*. **2013**, *1*, 4281–4288.

[24] Yang, M.; Song, Y.; Zhang, D.; Lin, S.; Hao, Z.; Liang, Y.; Zhang, D.; Chen, P. Converting a solvatochromic fluorophore into a protein-based pH indicator for extreme acidity. *Angew. Chem. Int. Ed*. **2012**, *51*, 7674–7679.

[25] Sim, J.; Kwon, D. S.; Kim, J. Acid-sensitive pH sensor using electrolysis and a microfluidic channel for read-out amplification. *RSC Adv.* **2014**, *4*, 39634–39638.

[26] Chen, L.; Wu, J.; Schmuck, C.; Tian, H. A switchable peptide sensor for real-time lysosomal tracking. *Chem. Commun*. **2014**, *50*, 6443–6446.

[27] Zhao, B.; Xu, Y.; Fang, Y.; Wang, L.; Deng, Q. Synthesis and fluorescence properties of phenanthro[9,10-*d*]imidazole derivative for Ag^{+} in aqueous media. *Tetrahedron Lett.* **2015**, *56*, 2460–2465.